Neurochem Res (2016) 41:1559–1569
DOI 10.1007/s11064-016-1869-1

ORIGINAL PAPER

Trimethyltin Modulates Reelin Expression and Endogenous Neurogenesis in the Hippocampus of Developing Rats

Amelia Toesca[1] · Maria Concetta Geloso[1] · Adriana Maria Mongiovì[1] · Alfredo Furno[1] · Arcangelo Schiattarella[2] · Fabrizio Michetti[1] · Valentina Corvino[1]

Received: 7 October 2015 / Revised: 22 January 2016 / Accepted: 10 February 2016 / Published online: 25 February 2016

Abstract Reelin is an extracellular matrix glycoprotein involved in the modulation of synaptic plasticity and essential for the proper radial migration of cortical neurons during development and for the integration and positioning of dentate granular cell progenitors; its expression is down-regulated as brain maturation is completed. Trimethyltin (TMT) is a potent neurotoxicant which causes selective neuronal death mainly localised in the CA1-CA3/hilus hippocampal regions. In the present study we analysed the expression of reelin and the modulation of endogenous neurogenesis in the postnatal rat hippocampus during TMT-induced neurodegeneration (TMT 6 mg/kg). Our results show that TMT administration induces changes in the physiological postnatal decrease of reelin expression in the hippocampus of developing rats. In particular, quantitative analysis of reelin-positive cells evidenced, in TMT-treated animals, a persistent reelin expression in the stratum lacunosum moleculare of Cornu Ammonis and in the molecular layer of Dentate Gyrus. In addition, a significant decrease in the number of bromodeoxyuridine (BrdU)-labeled newly-generated cells was also detectable in the subgranular zone of P21 TMT-treated rats compared with P21 control animals; no differences between P28 TMT-treated rats and age-matched control group were observed. In addition the neuronal commitment of BrdU-positive cells appeared reduced in P21 TMT-treated rats compared with P28 TMT-treated animals. Thus TMT treatment, administrated during development, induces an early reduction of endogenous neurogenesis and influences the hippocampal pattern of reelin expression in a temporally and regionally specific manner, altering the physiological decrease of this protein.

Keywords Trimethyltin · Hippocampal neurodegeneration · Reelin · Endogenous neurogenesis · Brain development

Introduction

Reelin is a large glycoprotein associated with the extracellular matrix, secreted by different neuronal cell populations, in particular Cajal-Retzius (CR) cells and GABAergic interneurons, in the developing, postnatal and adult mammalian brain [1]. During development, reelin is required for the proper radial migration of post-mitotic neurons in the cerebral and cerebellar cortex, contributing to correct layering of these structures and the formation of layer-specific connections [2–5]. During embryonic and early postnatal development, reelin is expressed in CR until the second postnatal week, when most CR cells undergo neuronal death [6–8]. Indeed it is well known that its expression is down-regulated as brain maturation is completed [8, 9]. Interestingly, in postnatal and adult human and rodent hippocampus, reelin is mainly synthesised and released by a subset of GABAergic interneurons belonging to a new generation of neurons that did not express reelin during development, suggesting a dynamic regulation of this protein [7].

Fabrizio Michetti and Valentina Corvino share the senior position.

✉ Fabrizio Michetti
fabrizio.michetti@unicatt.it

✉ Valentina Corvino
valentina.corvino@unicatt.it

[1] Institute of Anatomy and Cell Biology, Università Cattolica del Sacro Cuore, Largo Francesco Vito 1, 000168 Rome, Italy

[2] Institute of Biochemistry and Clinical Biochemistry, Università Cattolica del Sacro Cuore, Largo Francesco Vito 1, 000168 Rome, Italy

In adults, reelin enhances cell migration and synaptogenesis and is involved in a signalling pathway which underlies neurotransmission, memory formation and synaptic plasticity [10, 11].

It may be noteworthy in this respect that reelin expression is altered in a variety of neurologic and psychiatric disorders, such as temporal lobe epilepsy, schizophrenia, autism [10, 12–16].

Reelin has also been suggested to regulate neonatal and adult hippocampal neurogenesis, likely acting as guidance cue for the dentate granular cell progenitors [11, 17–19]. In addition, in vitro experiments hypothesised an association between reelin expression, neural stem cell proliferation and neurosphere formation [20].

The modulation of endogenous neurogenesis seems to be included in wider brain response mechanisms to the injury, likely under the control both of cell-intrinsic and extrinsic molecules, which still deserve investigation [21].

Organotins, such as trimethyltin (TMT) and triethyltin (TET), are a group of organometallic compounds based on tin with hydrocarbon substituents, exhibiting potent neurotoxicant effects [22–25]. However, despite their similar chemical structural features, they exhibit different patterns of toxicity [22–24]. TET mainly affects white matter inducing myelin vacuolation and central edema accompanied by impaired neuromotor function [22–24]; on the contrary, TMT causes neuronal death selectively localised in the limbic system. For this reason, it is widely used to obtain animal models of neurodegeneration and temporal lobe epilepsy associated with cognitive impairments and behavioural alterations [25, 26].

In both developing and adult rat brain, TMT-induced neurodegeneration is characterised by a massive loss of pyramidal neurons localised in the CA3/hilus and CA1 hippocampal subfields, accompanied by reactive astrogliosis and microglia activation, with sparing of calretinin- and parvalbumin -IR interneuron subpopulations [27–35]. Generally, TMT has not been found to induce myelin damage in rodents [23] and, in the developing rat, it does not modify the concentration or protein composition of isolated myelin [36]. In order to explore further the phenomena accompanying neurodegenerative processes during development, the present study examines the expression and distribution of reelin and the modulation of endogenous neurogenesis in the hippocampus of developing rat treated with the neurotoxicant TMT.

Materials and Methods

Animal Treatment

Wistar rat pups, derived from 6 litters, served as subjects. On the day of birth, litters were culled randomly to preserve eight pups per litter and randomly assigned to control or TMT treatment. Since the sensitivity to TMT of the CA pyramidal neurons is age-dependent, developing, in rats, in concomitance with their functional maturation 7 days after birth, at postnatal day 7 (P7) the animals were given a single i.p. injection of saline or TMT chloride (Sigma, St. Louis, MO, USA) dissolved in saline at a dose of 6 mg/kg body weight in a volume of 1 ml/kg body weight, as previously described [31, 36, 37]. Nine days after TMT intoxication, the animals intended for the study of endogenous neurogenesis were given an i.p. injection of bromodeoxyuridine (BrdU) (50 mg/kg dissolved in a saline solution 0.1 M NH4OH) once a day for three consecutive days. Control rats were treated with the same doses of BrdU.

Control and TMT-treated rats, intended for immunohistochemistry or Real Time PCR analysis, were sacrificed 14 (P21) days, when neuronal damage is clearly detectable and neurodegeneration is still progressive, or 21 (P28) days after TMT-treatment when the maximum severity of TMT-induced hippocampal damage is observed [38].

For histochemical and immunohistochemical analysis the animals ($n = 4$ for each group), under ketamine and diazepam (1:1 i.p.) anaesthesia, were perfused through the aorta with 50–100 ml of saline solution, followed by 100–150 ml of 0.01 M, pH 7.4, phosphate-buffered saline (PBS) and 4 % paraformaldehyde. Serial 40-µm coronal sections were cut on a freezing microtome, collected in cold PBS and processed for Nissl histochemical staining or for immunohistochemistry. The animals ($n = 3$ for each group) intended for Real Time PCR experiments were sacrificed by decapitation under anaesthesia, ketamine and diazepam (1:1 i.p.); the hippocampi were removed and processed for RNA extraction.

All the animal experimental procedures were approved by the Animal Experimentation Committee of the Università Cattolica del S. Cuore. All efforts were made to minimise animal suffering and to reduce the number of animals used. ARRIVE guidelines were followed.

RNA Isolation

Total RNA from hippocampus of saline solution or TMT treated animals, at 15 (P21) and 21(P28) days after treatment, was extracted using the TRIZOL reagent (Invitrogen, Carlsbad, CA, USA) according to the manufacturer's protocol. All samples were treated with DNaseI to remove residual genomic DNA in the RNA preparation. The yield of RNA isolation was determined using spectrophotometry (Beckman DU800; Beckman Coulter Inc.). The integrity of total RNA was assessed using Agilent 2100 Bioanalyzer (Agilent Technologies, Santa Clara, CA, USA).

Real-Time PCR

Reverse transcription (RT) was performed in 20 µl reactions containing 2 µg total RNA with SuperScript™ III First-Strand Synthesis System (Invitrogen, Carlsbad, CA, USA) using random hexamers, following the manufacturer's instructions. To rule out genomic DNA contamination, no-reverse controls (i.e., RT reactions carried out in the absence of the reverse transcriptase enzyme) were added for each sample. Thereafter, 1 µL of a 1:5 dilution of the single-stranded cDNA was used for real-time PCR, performed in a reaction volume of 20 µL using the SYBR green PCR master mix (Applied Biosystem, Foster City, CA, USA). Primers for real-time PCR were as follows: GAPDH_F, 5′-ctgaggaccaggttgtctcc-3′; GAPDH_R, 5′-ggaagaatgggagttgctgt-3′; reelin_F, 5′-tggagtttttaccccaatgc-3′; reelin_R, 5′-aggatggattgccacagaac-3′: The analysis was performed on an ABI Prism 7900 Sequence Detection System (Applied Biosystem) as follows: 10 min incubation at 95 °C followed by 40 cycles at 94 °C for 15 s and 60 °C for 1 min. All reactions were performed in triplicate. Standard curves were generated for all the assays to verify PCR efficiency. GAPDH mRNA was used as an internal control to correct for potential variation in RNA loading or efficiency of the amplification. Reelin expression was normalized to the GAPDH expression by calculating the ΔCt = (Ct of reelin - Ct of GAPDH). The ΔCt values were used for statistical analysis. The amplified transcripts were quantified using the comparative Ct method, with the formula for relative Fold Change (FC) = $2^{-\Delta\Delta Ct}$ [39].

Immunohistochemistry

Sections for reelin immunohistochemistry were incubated by free floating with mouse anti-reelin antibody (1:2000; Chemicon, Tamecula, CA, USA) overnight at 4 °C. For BrdU labeling, sections were first incubated, by free floating, with 2 N HCl at 37 °C for DNA denaturation (30 min), followed by 5 % normal goat serum at 37 °C (15 min) and then overnight with rat monoclonal anti-BrdU antibody (1:1000; Abcam, Cambridge, UK). The reactions were developed with the avidin–biotin peroxidase complex (ABC method, Vector Burlingame, CA) using 3,3′-diaminobenzidine (Sigma, St. Louis, MO) as chromogen.

After reelin or BrdU labeling, the sections were examined under a Zeiss Axiophot microscope (Carl Zeiss, Germany). Light microscopy images were captured on an Axiophot microscope equipped with a digital camera (AxioCam MRc) and image analysis software (Axiovision) (Carl Zeiss, Germany).

The neuronal differentiation fate of neural stem cells was analysed by double labeling with antibodies directed against the proliferation marker BrdU and the immature neuronal marker Doublecortin (DCX) (polyclonal, 1:3000, overnight at 4 °C, Chemicon, Temecula, CA). The reactions were revealed using secondary anti-guinea pig cyanine-3-conjugated antibody (Cy3, 1:400, 1 h at room temperature, Jackson Immunoresearch Laboratories, West Grove, PA) for DCX detection, while BrdU-labeling was revealed with secondary anti-rat FITC-conjugated antibody (1:200, 1 h at room temperature, Vector, UK).

The colocalization of two different markers was examined with a Zeiss LSM 510 META confocal laser scanning microscopy system.

Quantitative Analysis

Quantitative analysis of subgranular zone (SGZ) BrdU-positive cells and of reelin-immunoreactive (IR) cells present in the different subfields of rat hippocampus (namely CA1, CA2, CA3 stratum oriens (SO), CA1, CA2, CA3 stratum radiatum (SR), CA1, CA2, CA3 pyramidal layer (SP), CA1, CA3 stratum lacunosum moleculare (SLM), molecular layer (ML) of dentate gyrus (DG), SGZ and hilus) was performed as previously described [29–31, 40–42]. Estimates of the total number of cells positive for each marker were obtained using the following formula: $E = k \Sigma N$, where E is the estimate of the total number of counted cells in each case, ΣN is the sum of n values in the n ($n = 6$) sections considered, and k indicates that one section out of every k will be used ($k = 6$). N was corrected according to Abercrombie's formula: $N = n\ t/(t + D)$, where n is the number of cells counted in each section, t is the section thickness, and D is the mean diameter of the cells as previously described [29–31, 41, 42].

Quantitative analysis of DCX/BrdU double-labeled cells were quantified using z-scan confocal microscopy (Zeiss LSM 510 confocal-laser scanning microscope equipped with an Argon and He/Ne laser) at 40× magnification through the septo-temporal axis of the hippocampus in 1-in-12 series of sections, as previously described [42–44]. BrdU/DCX-double-stained cells were quantified in the entire length of the DG (upper and lower blades) [42]. All counts were performed using multi-channel configuration. Each cell was manually examined in its full z dimension and only those cells for which the nucleus was unambiguously associated with the lineage-specific marker were scored as positive.

The quantification of double-stained cells was expressed as the percentage of BrdU/DCX-positive cells in relation to the total number of BrdU-positive cells.

Statistical Analysis

Three-way Repeated-Measures (RM) ANOVA with TMT treatment (TMT-treated rats versus saline-treated rats) and

time (P21 versus P28) as the between-subjects factors and hippocampal subfields as the within-subjects factor, or two-way ANOVA with TMT treatment and time as main factors were performed to analyze statistically significant differences among different experimental groups. Data analysis was performed with StatView Software. When appropriate, post hoc comparisons were made using Tukey's-HSD test, with a significance level of $p < 0.05$.

In order to assess the statistical significance of the gene expression changes for each gene in each experimental group, an unpaired t test was used to compare the ΔCt values across the replicates, setting the p value cut-off at 0.05. Comparisons were made across all four experimental groups.

Results

Histological Analysis of Nissl-Stained Hippocampal Sections

Light microscopic analysis of Nissl-stained hippocampal sections showed moderate to severe neuronal loss mainly localised in the CA3 region and hilus of rats treated with TMT early during development, as already described [31] (Fig. 1). Treated animals, sacrificed 14 (Fig. 1b) and 21 (Fig. 1d) days after TMT intoxication, exhibited a progressive worsening of hippocampal neuronal loss that reached maximum severity 21 days after TMT administration (Fig. 1d).

Hippocampal Reelin mRNA Expression in Control and TMT-Treated Developing Rats

In controls, real time PCR revealed a significant down-regulation of reelin mRNA levels in the hippocampus of P28 rats compared whit P21 rats ($p < 0.05$), as expected [9]. On the contrary, in TMT-treated rats, reelin mRNA expression remained almost unmodified at both time points considered ($p > 0.05$) (Fig. 2). In addition, reelin mRNA levels in the hippocampus of P28 control rats were significantly down-regulated compared with all TMT-treated groups ($p < 0.05$) (Fig. 2).

Distribution Pattern and Quantitative Analysis of Reelin-Immunoreactive Cells in the Hippocampus of Control and TMT-Treated Developing Rats

Reelin-immunoreactive cells were distributed throughout all hippocampal subfields exhibiting essentially the same distribution pattern in all experimental groups (P21control and TMT-treated; P28 control and TMT-treated) (Fig. 3a–d). In particular, in the Cornu Ammonis several reelin-positive cells were present in the SO, scattered reelin-IR-cells were detected in the SR and only rare immunolabeling was found in the SP; numerous reelin-IR cells were present in the SLM mainly located near the hippocampal fissure (Fig. 3a–d). In the DG, several reelin-positive cells were present in the hilus and SGZ, while there was no labeling in the granular cell layer (Fig. 3a–d). Many reelin–IR neurons were detected in the ML of DG, especially in the outer part near the hippocampal fissure (Fig. 3a–d) reflecting the cell distribution already described [6, 7, 45].

Quantitative analysis, followed by three-way RM ANOVA, evidenced a significant age-dependent decrease in the number of reelin-IR cells in control animals in specific hippocampal subfields namely in the CA1 SO, in the CA1 SLM and in the ML of DG, in agreement with the physiological decrease of this protein described elsewhere (Fig. 3e); conversely, in TMT-treated rats, the expression of reelin remained essentially stable at the two time points considered. These data essentially confirm results obtained by real time PCR mRNA analysis.

In particular a significant TMT*time*hippocampal subfields interaction ($F_{10,120} = 3.1$), TMT*time interaction ($F_{1,12} = 5.9$), TMT*hippocampal subfields interaction ($F_{10,120} = 14.4$), time*hippocampal subfields interaction ($F_{10,120} = 6.56$) were revealed; time ($F_{1,12} = 7$) and hippocampal subfields ($F_{10,120} = 120$) effects were also significant. Tukey's-HSD post hoc test indicated a significant decrease in reelin immunoreactivity in the ML of DG ($p < 0.001$) and in the CA1 SLM ($p < 0.001$) of P28 control group compared with P21 control animals (Fig. 3e, f); the ML of P28 control group also showed a significantly lower number of reelin-IR cells compared with both TMT-treated groups ($p < 0.001$) (Fig. 3e). No significant differences were detectable between the TMT-treated groups at the two time points considered both in ML and in CA1 SLM.

A significant reduction in the number of reelin-IR cells was also evident in the CA1 SO of P28 control rats compared with P21 control animals ($p < 0.001$); the number of reelin-IR cells in P21 control rats was also higher than both TMT-treated groups (Fig. 3g; $p < 0.001$), while no differences were appreciable between TMT-treated groups and between P28 TMT and age-matched control group (Fig. 3g).

No significant change in the number of reelin-IR-cells was present in the other hippocampal layers examined among the four experimental groups (data not shown).

Effects of TMT-Treatment on Hippocampal Neurogenesis in Developing Rats

Light microscopy analysis of BrdU-labeled sections revealed the presence of many round shaped nuclei localised in the SGZ hippocampal region of all experimental groups,

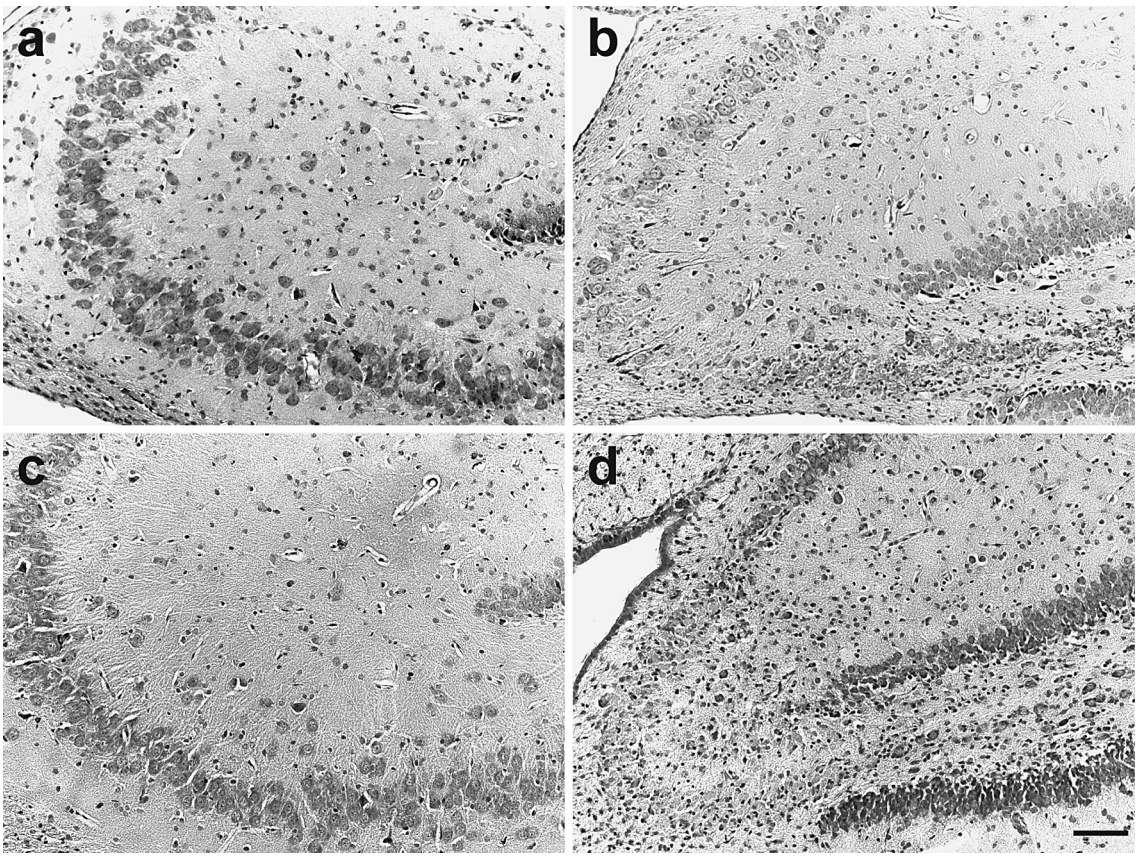

Fig. 1 **a**–**d** Micrographs of hippocampal CA3/hilus Nissl-stained sections of P21 (**a**, **b**) and P28 rats (**c**, **d**) treated with saline (**a**, **c**) or TMT (**b**, **d**) and sacrificed 14 days (**a**, **b**) or 21 days after treatment (**c**, **d**). Moderate to severe neuronal loss is evident in TMT-treated animals (**b**, **d**). *Scale bar* 150 μm

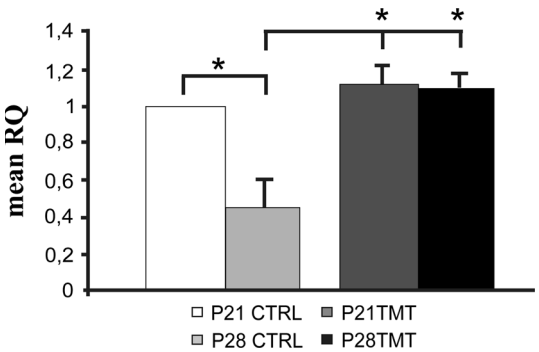

Fig. 2 *Bar graphs* represent results of quantitative real time-PCR obtained using the ΔΔCt method to calculate the relative quantity (RQ) of reelin gene at the tested time points. The values are given as mean ± SD; *$p < 0.05$

exhibiting features of newly generated cells [40, 46] (Fig. 4). A higher number of BrdU-IR cells was evident in P21 control group compared with P21 TMT-treated rats (Fig. 4a, b).

Two way ANOVA showed a significant effect of TMT-treatment ($F_{1,12} = 19{,}22$) and a significant TMT-treatment*time interaction ($F_{1,12} = 6{,}4$) (Fig. 4e).

Tukey's-HSD post hoc test evidenced a significant higher number of BrdU-positive cells in P21 control rats compared with P21 and P28 TMT-treated animals ($p < 0.05$). At the later time point, in P28 control rats the number of BrdU-labeled cells declined, in line with previous reports [47–51], although this reduction did not reach a statistically significant level ($p > 0.05$) (Fig. 4e). Furthermore, in P28 TMT-treated group the number of BrdU-positive cells remained substantially unchanged compared with age-matched control group and with P21 TMT-treated-rats ($p > 0.05$) (Fig. 4e).

Confocal microscope analysis of BrdU/DCX double-stained cells, performed to explore the neuronal commitment of proliferating cells, evidenced numerous BrdU/DCX double-stained cells, mainly located in the SGZ of both control (Fig. 5a, c) and TMT-treated animals (Fig. 5b, d).

Possible differences in the percentage of BrdU/DCX-double-labeled cells among the different experimental groups were also evaluated. Quantitative analysis of double labeled cells followed by two Way ANOVA revealed a significant time effect ($F_{1\text{-}15} = 6{,}9$ $p < 0.05$). Unpaired t-student test showed a significant increase in the

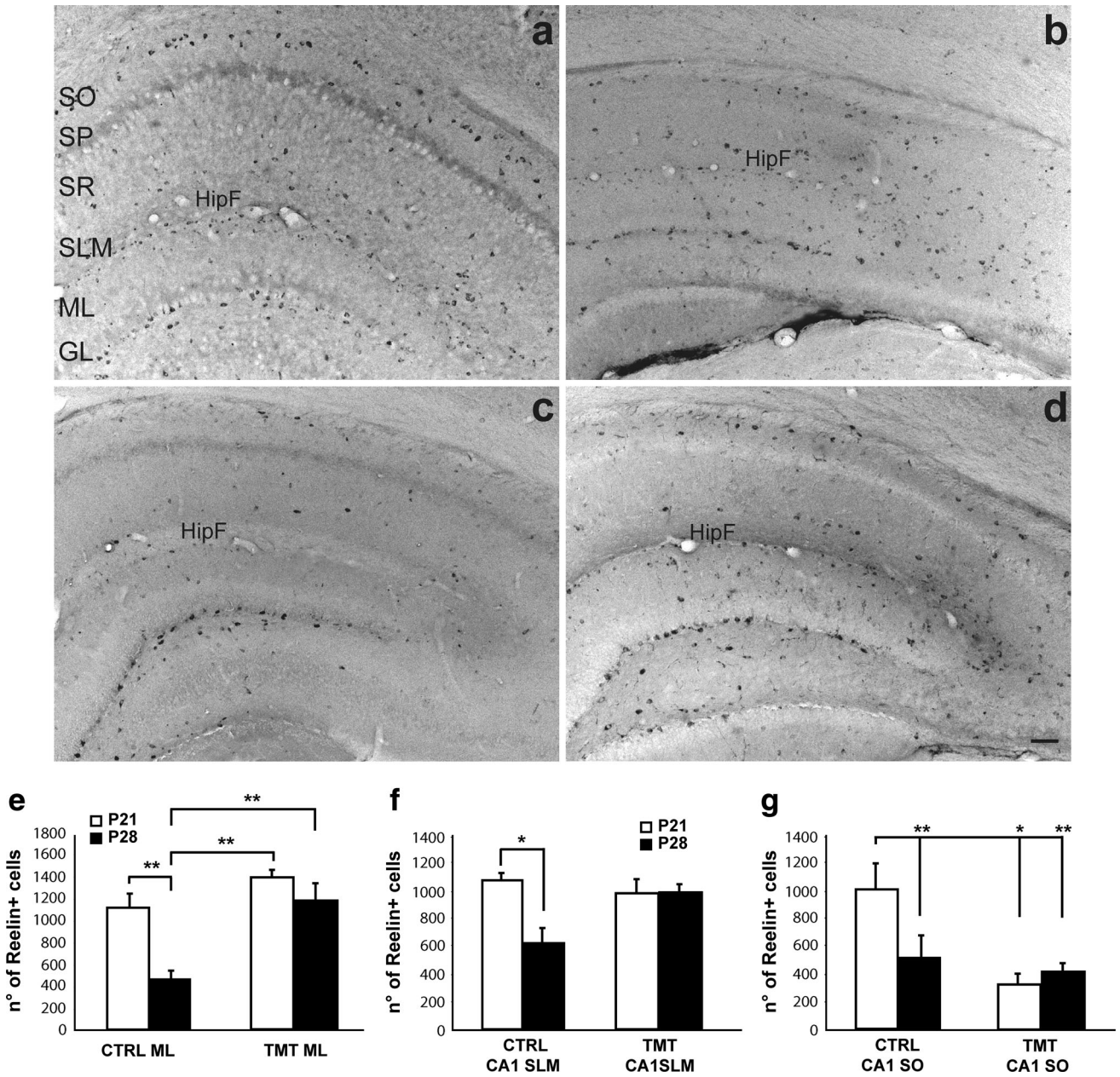

Fig. 3 **a**–**d** Reelin-stained hippocampal sections from developing rat hippocampi at postnatal ages P21 (**a**, **b**) and P28 (**c**, **d**) treated with saline (**a**, **c**) or TMT (**b**, **d**). The presence of many reelin-positive cells is evident in the stratum oriens (SO) of CA1 of P21 control rats (**a**) compared with P21 TMT-treated rats (**b**). A marked decrease in reelin immunoreactivity is detectable in the stratum lacunosum-moleculare (SLM) and in the molecular layer (ML) of P28 control rats (**c**) compared with P21 control rats (**a**); a smaller amount of reelin-IR cells can be observed in the ML of P28 control group (**c**) compared with both TMT-treated groups (**b**, **d**). *GL* granular layer, *SP* pyramidal layer, *SR* stratum radiatum, *HipF* hippocampal fissure. *Scale bar* 100 μm. **e**–**g** Number of reelin-IR cells in the ML (**e**), in the CA1 SLM (**f**) and in the CA1 SO (**g**) of developing rats at postnatal ages P21 and P28 treated with saline or TMT. A significant decrease in the number of reelin-IR cells is detectable in P28 control rats compared with P21 control rats in the ML, in the CA1 SLM and in the CA1 SO (**e**, **f**, **g**). The number of reelin-IR cells is also significantly reduced in the ML of P28 control group compared with both TMT-treated groups (**e**). A significantly higher number of reelin-IR cells is evident in the CA1 SO of P21 control rats compared with both TMT-treated groups (**g**).The values are given as mean ± SD; $^{*}p < 0.05$, $^{**}p < 0.001$

percentage of BrdU/DCX co-expressing cells in P28 TMT-treated rats compared with P21 TMT-treated animals ($p < 0{,}05$) while no difference in the percentage of BrdU/DCX double-labeled cells between control groups ($p > 0{,}05$) at two time points considered was detectable (Fig. 5e).

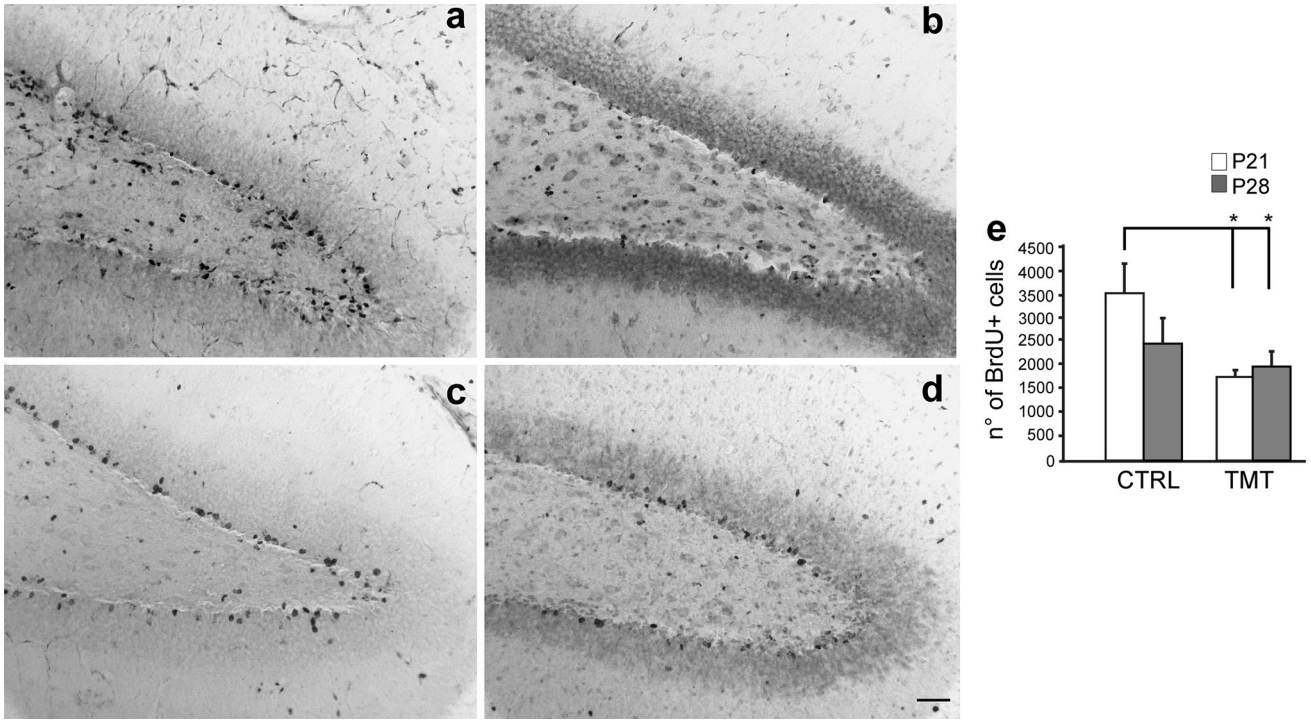

Fig. 4 **a**–**d** BrdU-stained sections from the hippocampus of developing rats at postnatal ages P21 (**a**, **b**) and P28 (**c**, **d**) treated with saline (**a**, **c**) or TMT (**b**, **d**). A higher number of BrdU-IR cells is evident in the SGZ of P21 control rats compared with P21TMT-treated rats. *Scale bar* 90 μm. **e** Number of BrdU-stained nuclei in the SGZ hippocampal region. The number of BrdU-positive cells is significantly higher in P21 treated animals compared with both P21 and P28 TMT-treated rats. The values are given as means ± S.D. (*$p < 0.05$)

Discussion

In the present study we examined the neurodegenerative effects of TMT in the hippocampus of P21 and P28 rats, during a critical period in the rodent brain postnatal development when juveniles mature into young adults (postnatal week 2–5), and when insults can have dramatic consequences as cognitive impairments and developmental disorders [52–54]. Our data showed that TMT-induced hippocampal degeneration in developing rats influences the hippocampal pattern of reelin expression, in a temporally and regionally specific manner, altering its physiological decrease [7], and modulates the endogenous neurogenesis, reducing the number of newly-generated cells.

In particular, our findings highlight a persistent reelin expression near the hippocampal fissure, in the SLM of CA1 and in the ML of DG of P28 TMT-treated animals. These data are in line with results obtained in the experimental model of developmental temporal lobe epilepsy induced by intra-hippocampal kainic acid (KA) injection showing a selective sparing of reelin expressing neurons along the hippocampal fissure [55].

It appears to be especially striking that, in TMT-model, the observed persistence of reelin-IR cells corresponds to areas that are main targets of the entorhinal-hippocampal pathway, namely ML of DG and SLM [3, 4]. In the early postnatal hippocampus, reelin is greatly secreted by CR cells in these subfields, being also required for the correct targeting, growth and branching of entorhinal afferents [2, 11].

Thus, bearing in mind that TMT causes neuronal loss in other limbic structures, especially pyriform/entorhinal cortex [28, 38], whose destruction leads to hippocampal deafferentation [56], the possibility that the prolonged expression of reelin may be in connection with deafferentation processes caused by TMT-administration should be considered. The lack of reelin physiological decrease could be a part of the response triggered by neurodegenerative processes and by disruptions in hippocampal architecture induced by TMT treatment, which modulates both the events associated with synaptic plasticity [56] and reorganisation of the neuronal network.

Interestingly, while reelin expression was globally preserved in the TMT-treated hippocampus, a significant reduction in the number of reelin-IR cells in CA1 SO of P21 TMT-treated rats compared with P21 control animals was observed. The early loss of this reelin-IR cell subpopulation could be related to their particular vulnerability; these cells are GABA-interneurons, which could play a role in neurodegenerative events, possibly involving seizure events, as already hypothesized in the pilocarpine model of experimental epilepsy, in

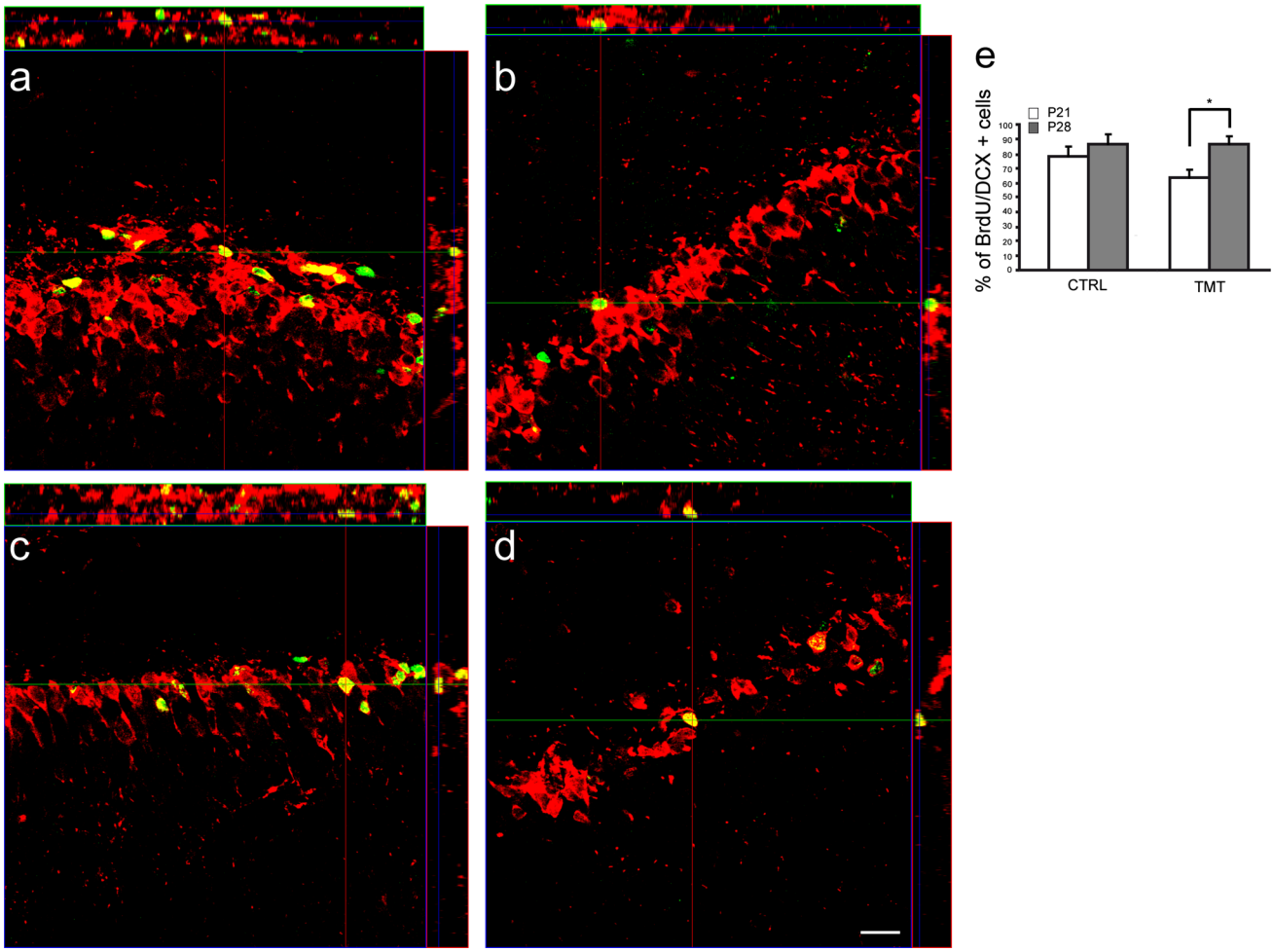

Fig. 5 **a**–**d** Representative confocal microscopy micrographs of P21 (**a**, **b**) and P28 (**c**, **d**) dentate sections of control (**a**, **c**) and TMT–treated (**b**, **d**) rats double-labeled for DCX (*red*) and BrdU (*green*). *Scale Bar* 60 μm. **e** The percentage of BrdU/DCX-double-labeled cells was significantly increased in P28 TMT-treated rats compared with P21 TMT-treated animals. The values are given as means ± S.D. (*$p < 0.05$) (Color figure online)

which a decline in GABA-interneuron subpopulations in the CA1 SO has been described [57].

TMT-induced modulation of hippocampal neurogenesis in developing rats shows features different from those described in the mature brain, in which an enhancement of dentate neurogenesis has been described [40]. Our results evidence an early reduction of newly generated cell proliferation in the SGZ of developing hippocampus in TMT treated rats, in line with data obtained in KA, flurothyl (bis-2,2,2-triflurothylether), pilocarpine models of experimental epilepsy [49, 58–60]. The mechanism that underlies the TMT effects on endogenous neurogenesis in developing rats could depend on age-related differences in the neurogenic response to damage. It may be relevant, in this respect, that the DG attains mature pattern later than other hippocampal regions (almost 1 month after birth) [61]; thus TMT treatment at P7 affects DG neurogenic niche in a critical developmental period in which newborn granule cells are still reaching their electrophysiological maturation [62–64].

On the contrary, at the later time point, in P28 TMT-treated group the number of BrdU-positive cells remains substantially unchanged compared to age-matched control and to P21 TMT-treated groups. Interestingly, a later increase in the percentage of mitotically active cells expressing immature neuronal marker DCX in P28 TMT-treated group compared with P21 TMT-treated animals has been observed.

These data may suggest that TMT induces an early reduction, followed by a quite steady-state level, of cell proliferation also accompanied by a delayed and stepwise commitment of newly-generated cells to neuronal fate; these events are possibly correlated to the morphological and neurochemical changes occurring within the damaged hippocampus.

Thus, the combined effects of different factors involved in the regulation of endogenous neurogenesis, such as

developmental stage, damage-triggered changes, neurogenic microenvironment, could result in an altered proliferation and differentiation of precursor cells in TMT-injured hippocampus.

Interestingly, the involvement of reelin in the modulation of hippocampal neurogenesis has been hypothesized [11, 18, 65–67]. Indeed, reelin is expressed predominantly in cells located in the SGZ near precursors cells, thus likely contributing to migration and maturation of newborn granular cells [17, 19]. However, the modulation of neurogenesis induced in developing rats by TMT treatment is not accompanied by a variation in the number of reelin-expressing cells in the SGZ, so that a direct interrelation among the levels of reelin and neurogenesis processes in the present experimental system cannot clearly be evidenced. These findings differ from data obtained both in human epileptic patients [14] and in some experimental models of epilepsy, in which a general reduction of reelin expression in the DG parallels (and is suggested to underlie) granule cell dispersion (GCD), usually observed in these hippocampal degenerative processes [14, 19, 68–70]. In TMT-induced neurodegeneration GCD is not observed [25, 38], possibly with a specific relation with the preserved expression of reelin described in this model.

To summarize, TMT treatment, administrated early during development, reduces endogenous dentate neurogenesis and influences the hippocampal pattern of reelin expression altering its physiological decrease. The present results hint at the possibility that both phenomena, in an integrated or distinct manner, might play a role in the tissue response to brain damage.

Acknowledgments This work was supported by funds from Università Cattolica del S. Cuore to A.T. and to F.M.

Compliance with Ethical Standards

Conflict of interest The authors declare no conflict of interest.

Reference

1. Frotscher M (2010) Role for reelin in stabilizing cortical architecture. Trends Neurosci 33:407–414
2. Del Rio JA, Heimrich B, Borrell V, Förster E, Drakew A, Alcántara S, Nakajima K, Miyata T, Ogawa M, Mikoshiba K, Derer P, Frotscher M, Soriano E (1997) A role for Cajal-Retzius cells and reelin in the development of hippocampal connections. Nature 385:70–74
3. Frotscher M (1997) Dual role of Cajal-Retzius cells and reelin in cortical development. Cell Tissue Res 290:315–322
4. Borrell V, Del Río JA, Alcántara S, Derer M, Martínez A, D'Arcangelo G, Nakajima K, Mikoshib K, Derer P, Curran T, Soriano E (1999) Reelin regulates the development and synaptogenesis of the layer-specific entorhino-hippocampal connections. J Neurosci 19:1345–1358
5. Borrell V, Pujadas L, Simó S, Durà D, Solé M, Cooper JA, Del Río JA, Soriano E (2007) Reelin and mDab1 regulate the development of hippocampal connections. Mol Cell Neurosci 36:158–173
6. Drakev A, Frotscher M, Deller T, Ogawa M, Heinrich B (1998) Developmental distribution of a reeler gene-related antigen in the rat hippocampal formation visulized by CR-50 immunocytochemistry. Neuroscience 82:1079–1086
7. Pesold C, Impagnatiello F, Pisu MG, Uzunov DP, Costa E, Guidotti A, Caruncho HJ (1998) Reelin is preferentially expressed in neurons synthesizing gamma-aminobutyric acid in cortex and hippocampus of adult rats. Proc Natl Acad Sci USA 95:3221–3226
8. Supèr H, Martínez A, Del Río JA, Soriano E (1998) Involvement of distinct pioneer neurons in the formation of layer-specific connections in the hippocampus. J Neurosci 18:4616–4626
9. Alcántara S, Ruiz M, D'Arcangelo G, Ezan F, de Lecea L, Curran T, Sotelo C, Soriano E (1998) Regional and cellular patterns of reelin mRNA expression in the forebrain of the developing and adult mouse. J Neurosci 18:7779–7799
10. Knuesel I (2010) Reelin-mediated signaling in neuropsychiatric and neurodegenerative diseases. Prog Neurobiol 91:257–274
11. Pujadas L, Gruart A, Bosch C, Delgado L, Teixeira CM, Rossi D, de Lecea L, Martínez A, Delgado-García JM, Soriano E (2010) Reelin regulates postnatal neurogenesis and enhances spine hypertrophy and long-term potentiation. J Neurosci 30:4636–4649
12. Fatemi SH, Earle JA, McMenomy T (2000) Reduction in reelin immunoreactivity in hippocampus of subjects with schizophrenia, bipolar disorder and major depression. Mol Psychiatry 5:654–663
13. Fatemi SH, Kroll JL, Stary JM (2001) Alterated levels of reelin and its isoforms in schizophrenia and mood disorders. NeuroRep 12:3209–3215
14. Haas CA, Dudeck O, Kirsch M, Huszka C, Kann G, Pollak S, Zentner J, Frotscher M (2002) Role for reelin in the development of granule cell dispersion in temporal lobe epilepsy. J Neurosci 22:5797–5802
15. Haas CA, Frotscher M (2010) Reelin deficiency causes granule cell dispersion in epilepsy. Exp Brain Res 200:141–149
16. Lakatosova S, Ostatnikova D (2012) Reelin and its complex involvement in brain development and function. Int J Biochem Cell Biol 44:1501–1504
17. Frotscher M, Haas CA, Förster E (2003) Reelin controls granule cell migration in the dentate gyrus by acting on the radial scaffold. Cereb Cortex 13:634–640
18. Won SJ, Kim SH, Xie L, Wang Y, Mao XO, Jin K, Greenberg DA (2006) Reelin-deficient mice show impaired neurogenesis and increased stroke size. Exp Neurol 198:250–259
19. Gong C, Wang TW, Huang HS, Parent JM (2007) Reelin regulates neuronal progenitor migration in intact and epileptic hippocampus. J Neurosci 27:1803–1811
20. Massalini S, Pellegatta S, Pisati F, Finocchiaro G, Farace MG, Ciafrè SA (2009) Reelin affects chain-migration and differentiation of neural precursor cells. Mol Cell Neurosci 42:341–349
21. Saha B, Jaber M, Gaillard A (2012) Potentials of endogenous neural stem cells in cortical repair. Front Cell Neurosci 6:14. doi:10.3389/fncel.2012.00014
22. Chang LW (1990) The neurotoxicology and pathology of organomercury, organolead, and organotin. J Toxicol Sci 15:125–151
23. O'Shaughnessy DJ, Losos GJ (1986) Peripheral and central nervous system lesions caused by triethyl- and trimethyltin salts in rats. Toxicol Pathol 14:141–148
24. Aschner M, Aschner JL (1992) Cellular and molecular effects of trimethyltin and triethyltin: relevance to organotin neurotoxicity. Neurosci Biobehav Rev 16:427–435

25. Geloso M, Corvino V, Michetti F (2011) Trimethyltin-induced hippocampal degeneration as a tool to investigate neurodegenerative processes. Neurochem Int 58:729–738
26. Corvino V, Marchese E, Michetti F, Geloso MC (2013) Neuroprotective strategies in hippocampal neurodegeneration induced by the neurotoxicant trimethyltin. Neurochem Res 38:240–253
27. Chang LW (1984) Trimethyltin induced hippocampal lesions at various neonatal ages. Bull Environ Contam Toxicol 33:295–301
28. Woodruff ML, Baisden RH (1990) Exposure to trimethyltin significantly enhances acetylcholinesterase staining in the rat dentate gyrus. Neurotoxicol Teratol 12:33–39
29. Geloso MC, Vinesi P, Michetti F (1996) Parvalbumin-immunoreactive neurons are not affected by trimethyltin-induced neurodegeneration in the rat hippocampus. Exp Neurol 139:269–277
30. Geloso MC, Vinesi P, Michetti F (1997) Calretinin-containing neurons in trimethyltin-induced neurodegeneration in the rat hippocampus: an immunocytochemical study. Exp Neurol 146:67–73
31. Geloso MC, Vinesi P, Michetti F (1998) Neuronal subpopulations of developing rat hippocampus containing different calcium-binding proteins behave distinctively in trimethyltin-induced neurodegeneration. Exp Neurol 154:645–653
32. Geloso MC, Corvino V, Cavallo V, Toesca A, Guadagni E, Passalacqua R, Michetti F (2004) Expression of astrocytic nestin in the rat hippocampus during trimethyltin-induced neurodegeneration. Neurosci Lett 357:103–106
33. Pompili E, Nori SL, Geloso MC, Guadagni E, Corvino V, Michetti F, Fumagalli L (2004) Trimethyltin-induced differential expression of PAR subtypes in reactive astrocytes of the rat hippocampus. Brain Res Mol Brain Res 122:93–98
34. Latini L, Geloso MC, Corvino V, Giannetti S, Florenzano F, Viscomi MT, Michetti F, Molinari M (2010) Trimethyltin intoxication up-regulates nitric oxide synthase in neurons and purinergic ionotropic receptor 2 in astrocytes in the hippocampus. J Neurosci Res 88:500–509
35. Reali C, Scintu F, Pillai R, Donato R, Michetti F, Sogos V (2005) S100b counteracts effects of the neurotoxicant trimethyltin on astrocytes and microglia. J Neurosci Res 81:677–686
36. Miller DB, O'Callaghan J (1984) Biochemical, functional and morphological indicators of neurotoxicity: effects of acute administration of trimethyltin to the developing rat. J Pharmacol Exp Ther 231:744–751
37. Barone S Jr (1993) Developmental differences in neural damage following trimethyl-tin as demonstrated with GFAP immunohistochemistry. Ann N Y Acad Sci 679:306–316
38. Balaban CD, O'Callaghan JP, Billingsley ML (1988) Trimethyltin-induced neuronal damage in the rat brain: comparative studies using silver degeneration stains, immunocytochemistry and immunoassay for neurotypic and gliotypic proteins. Neuroscience 26:337–361
39. Livak KJ, Schmittgen TD (2001) Analysis of relative gene expression data using real-time quantitative PCR and the 2(-Delta Delta C(T)) method. Methods 25:402–408
40. Corvino V, Geloso MC, Cavallo V, Guadagni E, Passalacqua R, Florenzano F, Giannetti S, Molinari M, Michetti F (2005) Enhanced neurogenesis during trimethyltin-induced neurodegeneration in the hippocampus of the adult rat. Brain Res Bull 65:471–477
41. Corvino V, Marchese E, Zarkovic N, Zarkovic K, Cindric M, Waeg G, Michetti F, Geloso MC (2011) Distribution and time-course of 4-hydroxynonenal, heat shock protein 110/105 family members and cyclooxygenase-2 expression in the hippocampus of rat during trimethyltin-induced neurodegeneration. Neurochem Res 36:1490–1500
42. Corvino V, Marchese E, Giannetti S, Lattanzi W, Bonvissuto D, Biamonte F, Mongiovì AM, Michetti F, Geloso MC (2012) The neuroprotective and neurogenic effects of neuro peptide Y administration in an animal model of hippocampal neurodegeneration and temporal lobe epilepsy induced by trimethyltin. J Neurochem 122:415–426
43. Monie ML, Mizumatsu S, Fike JR, Palmer TD (2002) Irradiation induces neural precursor-cell dysfunction. Nat Med 8:955–962
44. Yang F, Wang JC, Han JL, Zhao G, Jiang W (2008) Different effects of mild and severe seizures on hippocampal neurogenesis in adult rats. Hippocampus 18:460–468
45. Ramos-Moreno T, Galazo MJ, Porrero C, Martìnez-Cerdeño V, Clasca F (2006) Extracellular matrix molecules and synaptic plasticity: immunomapping of intracellular and secreted Reelin in the adult rat brain. Eur J Neurosci 23:401–422
46. Kempermann G, Jessberger S, Steiner B, Kronenberg G (2004) Milestones of neuronal development in the adult hippocampus. Trends Neurosci 27:447–452
47. Kuhn HG, Dickinson-Anson H, Gage FH (1996) Neurogenesis in the dentate gyrus of the adult rat: age-related decrease of neuronal progenitor proliferation. J Neurosci 16:2027–2033
48. Dayer Alexandre G, Ford Abigail A, Kathryn M (2003) Short-term and long-term survival of new neurons in the rat dentate gyrus. J Comp Neurol 460:563–572
49. Dong H, Csernansky CA, Goico B, Csernansky JG (2003) Hippocampal neurogenesis follows kainic acid-induced apoptosis in neonatal rats. J Neurosci 23:1742–1749
50. Liu H, Kaur J, Dashtipour K, Kinyamu R, Ribak CE, Friedman LK (2003) Suppression of hippocampal neurogenesis is associated with developmental stage, number of perinatal seizure episodes, and glucocorticosteroid level. Exp Neurol 184(1):196–213
51. McDonald HY, Wojtowicz JM (2005) Dynamics of neurogenesis in the dentate gyrus of adult rats. Neurosci Lett 385:70–75
52. Dell'Anna E, Iuvone L, Calzolari S, Geloso MC (1997) Effect of acetyl-L-carnitine on hyperactivity and spatial memory deficits of rats exposed to neonatal anoxia. Neurosci Lett 223:201–205
53. Rice D, Barone S Jr (2000) Critical periods of vulnerability for the developing nervous system: evidence from humans and animal models. Environ Health Perspect 108:511–533
54. Speed HE, Dobrunz LE (2009) Developmental changes in short-term facilitation are opposite at temporoammonic synapses compared to Schaffer collateral synapses onto CA1 pyramidal cells. Hippocampus 19:187–204
55. Duveau V, Madhusudan A, Caleo M, Knuesel I, Fritschy JA (2011) Impaired reelin processing and secretion by Cajal-Retzius cells contributes to granule cell dispersion in a mouse model of temporal lobe epilepsy. Hippocampus 21:935–944
56. Koczyk D (1996) How does trimethyltin affect the brain: facts and hypotheses. Acta Neurobiol Exp 56:587–596
57. Cossart R, Dinocourt C, Hirsch JC, Merchan-Perez A, De Felipe J, Ben-Ari Y, Esclapez M, Bernard C (2001) Dendritic but not somatic GABAergic inhibition is decreased in experimental epilepsy. Nat Neurosci 4:52–62
58. McCabe BK, Silveira DC, Cilio MR, Cha BH, Liu X, Sogawa Y, Holmes GL (2001) Reduced neurogenesis after neonatal seizures. J Neurosci 21:2094–2103
59. Shi XY, Wang JW, Lei GF, Sun RP (2007) Morphological and behavioral consequences of recurrent seizures in neonatal rats are associated with glucocorticoid levels. Neurosci Bull 23:83–91
60. Xiu-Yu S, Ruo-Peng S, Ji-Wen W (2007) Consequences of pilocarpine-induced recurrent seizures in neonatal rats. Brain Dev 29:157–163
61. Bayer SA (1980) Development of the hippocampal region in the rat. II. Morphogenesis during embryonic and early post-natal life. J Comp Neurol 190:115–134

62. Liu X, Tilwalli S, Ye G, Lio PA, Pasternak JF, Trommer BL (2000) Morphologic and electrophysiologic maturation in developing dentate gyrus granule cells. Brain Res 856:202–212
63. Gould E, Cameron HA (1996) Regulation of neuronal birth, migration and death in the rat dentate gyrus. Dev Neurosci 18:22–35
64. Danzer SC (2008) Postnatal and adult neurogenesis in the development of human disease. Neuroscientist 14:446–458
65. Zhao S, Chai X, Frotscher M (2007) Balance between neurogenesis and gliogenesis in the adult hippocampus: role for reelin. Dev Neurosci 29:84–90
66. Teixeira CM, Martín ED, Sahún I, Masachs N, Pujadas L, Corvelo A, Bosch C, Rossi D, Martinez A, Maldonado R, Dierssen M, Soriano E (2011) Overexpression of Reelin prevents the manifestation of behavioral phenotypes related to schizophrenia and bipolar disorder. Neuropsychopharmacology 36:2395–2405
67. Teixeira CM, Kron MM, Masachs N, Zhang H, Lagace DC, Martinez A, Reillo I, Duan X, Bosch C, Pujadas L, Brunso L, Song H, Eisch AJ, Borrell V, Howell BW, Parent JM, Soriano E (2012) Cell-autonomous inactivation of the reelin pathway impairs adult neurogenesis in the hippocampus. J Neurosci 32:12051–12065
68. Heinrich C, Nitta N, Flubacher A, Müller M, Fahrner A, Kirsch M, Freiman T, Suzuki F, Depaulis A, Frotscher M, Haas CA (2006) Reelin deficiency and displacement of mature neurons, but not neurogenesis, underlie the formation of granule cell dispersion in the epileptic hippocampus. J Neurosci 26:4701–4713
69. Antonucci F, Di Garbo A, Novelli E, Manno I, Sartucci F, Bozzi Y, Caleo M (2008) Botulinum neurotoxin E (BoNT/E) reduces CA1 neuron loss and granule cell dispersion, with no effects on chronic seizures, in a mouse model of temporal lobe epilepsy. Exp Neurol 210:388–401
70. Müller MC, Osswald M, Tinnes S, Häussler U, Jacobi A, Förster E, Frotscher M, Haas CA (2009) Exogenous reelin prevents granule cell dispersion in experimental epilepsy. Exp Neurol 216:390–397